

Nanomaterials modified sensors for drug sensing



Thesis submitted in partial fulfillment for the
award of degree

Doctor of Philosophy

By

Vineet Kumar Mall

SCHOOL OF MATERIALS SCIENCE & TECHNOLOGY
INDIAN INSTITUTE OF TECHNOLOGY
(BANARAS HINDU UNIVERSITY)
VARANASI- 221005
INDIA

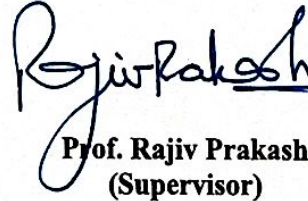
Roll No. 15111503

Year 2023

CERTIFICATE

It is certified that the work contained in the thesis titled "Nanomaterials modified sensors for drug sensing" by "Vineet Kumar Mall" has been carried out under my supervision and this work has not been submitted elsewhere for a degree.

It is further certified that the student has fulfilled all the requirements of Comprehensive, Candidacy, and SOTA.


25/11/2022

Prof. Rajiv Prakash
(Supervisor)
School of Materials Science & Technology,
Indian Institute of Technology,
Banaras Hindu University,
Varanasi-221005
Professor/आचार्य

School of Materials Science & Technology/पदार्थ विज्ञान एवं प्रौद्योगिकी स्कूल
Indian Institute of Technology/भारतीय प्रौद्योगिकी संस्थान
(Banaras Hindu University), Varanasi/काशी हिन्दू विश्वविद्यालय, वाराणसी

DECLARATION BY THE CANDIDATE

I, **Vineet Kumar Mall** certify that the work embodied in this thesis is my own bonafide work and carried out by me under the supervision of **Prof. Rajiv Prakash** from **December 2015 to November 2022** at the **School of Materials Science & Technology**, Indian Institute of Technology, Banaras Hindu University, Varanasi. The matter embodied in this thesis has not been submitted for the award of any other degree/diploma. I declare that I have faithfully acknowledged and given credits to the research workers wherever their works have been cited in my work in this thesis. I further declare that I have not willfully copied any other's work, paragraphs, text, data, results, etc., reported in journals, books, magazines, reports, dissertations, theses, etc., or available at websites and have not included them in this thesis and have not cited as my own work.

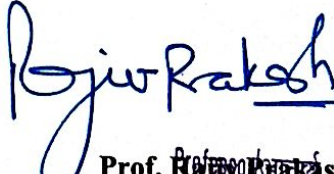
Date: 25.11.2022

Place: Varanasi


(Vineet Kumar Mall)

Certificate by the Supervisor

It is certified that the above statement made by the student is correct to the best of my knowledge.


25/11/2022
Prof. Rajiv Prakash
School of Materials Science & Technology
Indian Institute of Technology, Banaras Hindu University, Varanasi
IIT (BHU), Varanasi
(Banaras Hindu University), Varanasi/काशी हिन्दू विश्वविद्यालय, वाराणसी


Coordinator
School of Materials Science & Technology,
IIT (BHU), Varanasi
Coordinator/समन्वयक
School of Materials Science & Technology/पदार्थ विज्ञान एवं प्रौद्योगिकी स्कूल
Indian Institute of Technology/भारतीय प्रौद्योगिकी संस्थान
(Banaras Hindu University), Varanasi/काशी हिन्दू विश्वविद्यालय, वाराणसी

COPYRIGHT TRANSFER CERTIFICATE

Title of the Thesis: Nanomaterials modified sensors for drug sensing

Name of the Student: Vineet Kumar Mall

Copyright Transfer

The undersigned hereby assigns to the Indian Institute of Technology (Banaras Hindu University) Varanasi all rights under copyright that may exist in and for the above thesis submitted for the award of the "*Doctor of Philosophy*".

Date: 25.11.2022

Place: VARANASI


(Vineet Kumar Mall)

Note: However, the author may reproduce or authorize others to reproduce material extracted verbatim from the thesis or derivative of the thesis for the author's personal use provided that the source and the Institute's copyright notice are indicated.

Acknowledgement

I would like to extend my deepest sincerest gratitude to all the people who helped in any manner, who have shared the effort and knowledge in order to make this research a reality. Whatever has been accomplished and whatever has been the product of every endeavour, there is a great source of all effort, striving, guidance and gracious blessings without whom this task would have been impossible.

First and foremost, I would like to pay homage to the founder of Banaras Hindu University, Pandit Madan Mohan Malviya, who made this magnificent sanctuary to attain spiritual, intellectual, and scientific understanding of this huge cosmos.

*I would like to take this opportunity to offer my sincere gratitude to my respected supervisor **Professor Rajiv Prakash**, School of Materials Science & Technology, IIT (B.H.U.), Varanasi, for his unwavering support, insightful advice, and encouraging words throughout my time working with his research team. I was able to gain the knowledge of the topic because of his consistent encouragement, intellectual stimulation, astute advice, and incredibly valuable ideas and suggestions from the beginning to the end. I have been inspired by his thoughtful advice, wise cautions, intense interest, ongoing assistance, and kind demeanour.*

*I would like to express my sincere and wholehearted gratitude to **Prof. P. Maiti, Dr. A. K. Singh, Dr. C. Rath, Dr. C. Upadhyay, Dr. B. N. Pal, Dr. Ashish Kumar Mishra, Dr. Sanjay Singh, Dr. Shravan Kumar Mishra and Dr. Nikhil** (School of Materials Science and Technology, IIT-BHU, Varanasi) for discussion during seminars and valuable suggestions given by them. I am indeed obliged and sincerely thankful to my RPEC member **Prof. P. C. Pandey**, Department of Chemistry, IIT (B.H.U.) for his guidance and untiring attention right from the inception to the successful completion of assigned research work. Without close cooperation, most of the findings in this thesis would not have been possible. I am appreciative to the anonymous reviewers who repeatedly helped me by suggesting changes and guided me on my articles. Their feedback allowed me to improve articles by giving them a more polished finish.*

Acknowledgement

*My acknowledgement really deserves the special mention of my seniors in the lab who have taught me the lab culture and basic principles of the journey of research. I would like to acknowledge **Dr. Narsingh Raw Nirala, Dr. Uday Pratap Azad, Dr. Monika Srivastava, Dr. Ashish Kumar, Dr. Rajiv Kumar Pandey, Dr. Gopal Ji, Dr. Neeraj Giri, Dr. Sandeep Gupta, Dr. Madhu Tiwari, Dr. Kashish, Dr. Preeti Tiwari, Dr. Manish Kumar Singh and Dr. Richa Mishra, Dr. Vinita, Dr. Chandrajeet Verma** for all their support and motivation during the initial days of my PhD. I express my special thanks to **Dr. Preeti Tiwari** for her guidance, motivation and valuable suggestions. I convey my gratitude to my friend and lab mate **Dr. Ravi Prakash Ojha** for his unprecedented help and support during the tenure of my PhD.*

*Also, I am thankful to my lab fellows and juniors of my lab especially **Nikhil, Ajay, Aniruddha, Priya, Shweta, Subhajit, Saurabh, Rajpal, Shipra, Nupur, Radhe** for their helping behaviour. It's my fortune to gratefully acknowledge my research seniors and juniors from the Materials Science, **Dr. Satyaveer Singh, Dr. Arpan, Dr. Bishu Pada Majee, Dr. Ravi Prakash, Raman Hasariya, and Neela Pal** from the list is endless...thanks to one and all. Very special mention of my senior **Dr. Anil Kumar** (Department of Chemistry, B.H.U.) and my dear friends **Dr. Kshama Rai** (Department of Botany, B.H.U.) and **Dr. Omprakash** School of Materials Science & Technology, IIT (B.H.U.) who helped me directly or indirectly throughout the work. I am thankful to all non-teaching staff of SMST, IIT (BHU) and CIFIC for their cooperation at all levels.*

I gratefully acknowledge UGC, New Delhi for providing me with the necessary funding and fellowship to pursue the research work.

*I express my indebtedness to my parents **Smt. Raj Kumari Mall and Late Shri Ram Sanwer Mall** for their love, affection, and support during every moment of my life. This work would not have been possible without the grace of the "Maa Ganga and Baba Gangadhar".*

(Vineet Kumar Mall)

List of Figures

Figure No.	Figure Caption	Page No.
Figure 1.1	Schematic representation of a sensor with its various components	2
Figure 1.2	Pictorial representation of a) A three-electrode system and b) a two-electrode system	4
Figure 1.3	Amperometric titration apparatus for the determination of dissolved chlorine	6
Figure 1.4	Schematic representation of an electrochemical cell for voltammetric experiments	8
Figure 1.5	Classifications of Sensors	12
Figure 1.6	Schematic illustration of dimension-wise different categories of nanomaterials - zero (0D), one (1D), two (2D) and three dimensional (3D) with examples	19
Figure 1.7	Schematic representations of 2D nanomaterials	20
Figure 1.8	Structures of graphene, graphene oxide (GO) and reduced graphene oxide (RGO)	21
Figure 1.9	Representation of elements of the periodic table comprising TMDs	22
Figure 1.10	Schematic representation of sandwiched structure of 2D transition metal dichalcogenides (TMDs)	23
Figure 1.11	Schematic representation of work of Muduli et al., 2021	30
Figure 1.12	Schematic illustration of MoS ₂ -based simultaneous voltammetric determination of ascorbic acid (AA), dopamine (DA) and uric acid (UA)	34
Figure 1.13	Schematic representation of the fabrication of MoS ₂ /PANI/CPE and DPV response towards CAP detection	36
Figure 1.14	Schematic representation of the fabrication and sensing behaviour of Pd@rGO/MoS ₂ QDs modified GCE towards Nevirapine detection	38
Figure 1.15	Schematic representation of the preparation and sensing behaviour of	39

List of Figures

	MoS ₂ /PANI/fMWCNTsnanocompositemodified GCE	
Figure 2.1	A UV-visible spectrophotometer	47
Figure 2.2	Block diagram of a double beam UV-visible spectrophotometer	48
Figure 2.3	An FTIR spectrometer	49
Figure 2.4	Schematic representation of FTIR spectrophotometer	49
Figure 2.5	Schematic illustration of an X-ray beam getting diffracted by a crystallographic material	50
Figure 2.6	RigakuMiniFlexBenchtop 600 X-ray diffractometer	52
Figure 2.7	Schematic representation of the working of an X-ray Diffractometer	53
Figure 2.8	Basic principle involved in XPS	54
Figure 2.9	Schematic illustration of an XPS instrument	54
Figure 2.10	X-ray Photoelectron Spectrometer	55
Figure 2.11	Schematic illustration of signals emitted from different regions of the sample on interaction with electron beam	56
Figure 2.12	Block diagram of SEM	57
Figure 2.13	A Scanning Electron Microscope (SEM)	58
Figure 2.14	Schematic representation of a TEM instrument	59
Figure 2.15	Diagrammatic illustrations of Bright-field and Dark-field imaging	60
Figure 2.16	Transmission Electron Microscope	61
Figure 2.17	MetrohmAutolab (PGSTAT101, Netherlands)	62
Figure 2.18	a) CV input waveform and b) a general resulting output plot	63
Figure 2.19	Differential Pulse Voltammetry (DPV) - Pulse Sequence Detail	65
Figure 3.1	Schematic representation of the preparation of WS ₂ QDs	71
Figure 3.2	(a)FT-IR spectra and (b) UV-Vis. absorption spectra of WS ₂ QDs, rGO and rGO@WS ₂ QDs	73

List of Figures

Figure 3.3	Structural investigation by TEM a) rGO b) WS ₂ QDs and c) rGO@WS ₂ QDs (insets showing their corresponding SAED pattern)	75
Figure 3.4	EDAX spectra of a) rGO b) WS ₂ QDs and c) rGO@WS ₂ QDs	75
Figure 3.5	EDAX mapping for rGO@WS ₂ QDs (a) TEM image of information collection area, (b) overlap, (c) C element, (d) O element, (e) S element and (f) W element	76
Figure 3.6	CV response of different modified electrodes in phosphate buffer (pH 6) for 50 μM CQ at (a) bare GCE, (b) rGO modified GCE (c) WS ₂ QDs modified GCE and (d) rGO@WS ₂ QDs modified GCE.	77
Figure 3.7	CV response of (a) bare GCE and (b) rGO@WS ₂ QDs modified GCE at different scan rates: 10, 30, 50, 80, 100 mV/s, in 0.1 M phosphate buffer (pH 6) in presence of 50 μM CQ (c) Plot of anodic peak potentials vs. square root of scan rates for bare and rGO@WS ₂ QDs modified GCE.	78
Figure 3.8	CV curve (A) and its calibration plot (B) of rGO@WS ₂ QDs modified GCE in the presence of CQ (0.5 μM to 82.4 μM) in 0.1 M phosphate buffer at pH=6	80
Figure 3.9	DPV curve (A) and its calibration plot (B) of rGO@WS ₂ QDs modified GCE in the presence of CQ (0.5 μM to 82.4 μM) in 0.1 M phosphate buffer at pH=6	80
Figure 3.10	CV curve (A) and its calibration plot (B) of rGO@WS ₂ QDs modified GCE in the presence of CQ (0.5 μM to 82.4 μM) in human blood serum diluted with 0.1 M phosphate buffer at pH=6 in 1: 4 ratio	81
Figure 3.11	DPV curve (A) and its calibration plot (B) of rGO@WS ₂ QDs modified GCE in the presence of CQ (0.5 μM to 82.4 μM) in human blood serum diluted with 0.1 M phosphate buffer at pH=6 in 1: 4 ratio	81
Figure 3.12	CV curve (A) and its calibration plot (B) of	82

List of Figures

	rGO@WS ₂ QDs modified GCE in the presence of commercially available CQ tablet (0.5 μ M to 82.4 μ M) in 0.1 M phosphate buffer at pH=6	
Figure 3.13	DPV curve (A) and its calibration plot (B) of rGO@WS ₂ QDs modified GCE in the presence of commercially available CQ tablet (0.5 μ M to 82.4 μ M) in 0.1 M phosphate buffer at pH=6	82
Figure 3.14	Schematic representation of plausible mechanism for electrooxidation of CQ on rGO@WS ₂ QDs modified GCE	83
Figure 3.15	Interference studies of different biological species with CQ in the ratio of 10:1 by DPV in 0.1 M phosphate buffer at pH= 6.	84
Figure 3.16	(a) Intra-day study and (b) Inter-day study of developed electrochemical sensor by DPV in 0.1 M phosphate buffer at pH= 6 in presence of 50 μ M CQ.	85
Figure 4.1	Schematic presentation of synthesis of MoS ₂ nanosheets using hydrothermal technique.	92
Figure 4.2	Schematic illustration for the exfoliation of MoS ₂ nanosheet and synthesis of MoS ₂ -PIn nanocomposite	93
Figure 4.3	(a) XRD spectrum of MoS ₂ , CPIIn and MoS ₂ -CPIIn, (b) FTIR spectra of MoS ₂ , CPIIn and MoS ₂ -CPIIn, (c) XPS survey spectrum corresponding to MoS ₂ -CPIIn (d) displays the SEM image related to CPIIn, (e) MoS ₂ and (f) MoS ₂ -CPIIn, (g) TEM micrograph of MoS ₂ , (h) CPIIn and (i) MoS ₂ -CPIIn, Inset of g-i shows SAED pattern.	95
Figure 4.4	XPS spectra of MoS ₂ -CPIIn (a) C 1s, (b) N 1s, (c) O 1s (d) Mo 3d and (e) S 2p respectively.	98
Figure 4.5	CV curves of Azp (9.9 μ M) in 0.1 M PBS of pH 7.4 (a) without Azp and (b) with Azp at MoS ₂ -CPIIn/GCE	99
Figure 4.6	(a) CV of Azp (9.9 μ M) in 0.1 M PBS buffer over	101

List of Figures

	MoS ₂ -CPIIn modified GCE at different pH 6.4, 7.0, 7.4 and 8.0, (b) DPV of Azp (9.9 μM) in 0.1 M PBS buffer over MoS ₂ -CPIIn modified GCE at different pH 6.4, 7.0, 7.4 and 8.0.	
Figure 4.7	(a) CV plots of Azp (50 μM) in PBS buffer (pH 7.4; 0.1 M) over different electrodes, (b) DPV curves of Azp (50 μM) in PBS buffer (pH 7.4; 0.1 M) over different electrodes.	102
Figure 4.8	DPV measurements of various concentrations of Azp (3.49-284.44 μM) (a-r) using MoS ₂ -CPIIn modified GCE in PBS buffer (pH 7.4; 0.1M), (b) linear calibration plot of Azp in PBS buffer (pH 7.4; 0.1M). (c) DPV responses of different concentrations of Azp (4-98.29 μM) (a-r) using MoS ₂ -CPIIn modified GCE in human blood serum, (d) linear calibration plot of Azp in the human blood serum sample.	104
Figure 4.9	Interference study. The x axis denotes the tested compounds and the y axis denotes the interference effect in percentage (%).	107

Figure 5.1	Hydrothermal synthesis of MoS ₂ nanosheets	114
Figure 5.2	Preparation of GNR by seed-mediated growth methodology	115
Figure 5.3	Schematic pathway for the synthesis of GNR decorated MoS ₂ nanosheets (MoS ₂ -GNR)	116
Figure 5.4	(a) XRD spectra, (b) FTIR spectra of MoS ₂ , GNR and MoS ₂ -GNR	117
Figure 5.5	TEM micrograph of (a) MoS ₂ , (b) GNR and (c) MoS ₂ -GNR, and SAED pattern of (d) MoS ₂ , (e) GNR and (f) MoS ₂ -GNR	119
Figure 5.6	XPS characterization (a), XPS survey spectrum, the deconvoluted spectrum of Mo 3d, (b), S 2p (c), and Au 4f (d) regions of MoS ₂ -GNR	120

List of Figures

Figure 5.7	Cyclic voltammograms (a) and Nyquist plots (b) of composite samples 1:1, 1:5, 1:7, 1:10, and 1:30 in 5 mM $[\text{Fe}(\text{CN})_6]^{3-/4-}$ solution in PBS (pH 7.4)	121
Figure 5.8	Cyclic voltammograms (a) and Nyquist plots (b) of bare GCE, MoS_2 , GNR, and MoS_2 -GNR composite of 5 mM $[\text{Fe}(\text{CN})_6]^{3-/4-}$ in PBS (pH 7.4).	123
Figure 5.9	(a) CV and (b) Nyquist plots of PQ (50 μM) in 0.1 M PBS of pH 7.4 at bare GCE and MoS_2 -GNR modified GCE	125
Figure 5.10	(a) CV and (b) DPV of PQ (50 μM) in 0.1 M PBS on MoS_2 -GNR modified GCE at pH 5.0, 6.0, 7.0, 7.4, 9.0, and 10.0	127
Figure 5.11	(a) DPV measurements and (b) linear calibration plot of various concentrations of PQ (1-150 μM) (a-j) MoS_2 -GNR modified GCE in 0.1 M PBS (pH 7.4)	128
Figure 5.12	Interference study of potential interferents on the voltammetric response of 50 μM PQ. The interfering species concentration was 500 μM , and for PQ, it was 50 μM	129
Figure 5.13	Intra-day stability examination of the developed electrochemical sensor by DPV in 0.1 M PBS at pH 7.4 with 50 μM PQ	130
Figure 5.14	(a) DPV curves and (b) linear calibration plot of various concentrations of PQ (3.98-117.65 μM) (a-j) MoS_2 -GNR modified GCE in human blood serum samples	131

List of Tables

Table No.	Table Caption	Page No.
Table 1.1	Primary advantages and limitations of graphene and its derivatives	25
Table 1.2	2D nanocomposites in drug sensing applications	39
Table 3.1	Comparative study for electrochemical detection of Chloroquine based on earlier reported works	85
Table 4.1	DPV detection of Azp in spiked blood serum sample	105
Table 4.2	Comparison with earlier reported studies for electrochemical detection of Azp	105
Table 5.1	Comparison of values of R_{ct} in Nyquist plot and potential difference in CV redox peaks in 5 mM Ferri/Ferro solution in PBS regarding different samples of MoS ₂ - GNR	122
Table 5.2	Comparison of values of R_{ct} in Nyquist Plot, the potential difference in CV redox peaks, and oxidation and reduction peak currents in 5mM Ferri/Ferro solution in PBS regarding different prepared electrode materials	123
Table 5.3	DPV determination of PQ in spiked blood serum samples	132
Table 5.4	DPV determination of PQ in the tablet	133
Table 5.5	Comparison of electrochemical sensing works of PQ reported in the literature	133

LIST OF ABBREVIATIONS

μA	:	Microampere
μL	:	Microlitre
μM	:	Micromolar
ν	:	Scan rate
$^{\circ}\text{C}$:	Degree Celsius
0D	:	Zero dimensional
1D	:	One dimensional
2D	:	Two dimensional
3D	:	Three dimensional
CPIIn	:	Poly(5-carboxyindole)
A	:	Effective surface area
AA	:	Ascorbic acid
AC	:	Acetaminophen
AE	:	Auxiliary electrode
AIDS	:	Acquired Immuno Deficiency Syndrome
Ag NPs	:	Silver nanoparticles
APS	:	Ammonium persulphate
Aq.	:	Aqueous
Azp	:	Azathioprine
Au NPs	:	Gold nanoparticles
C	:	Concentration
CAP	:	Chloramphenicol
CAF	:	Caffeine
CDs	:	Carbon dots
5CIn	:	5-carboxyindole
cm	:	Centimeter

LIST OF ABBREVIATIONS

CNT	:	Carbon nano tube
Conc.	:	Concentrated
CPE	:	Carbon paste electrode
CPIIn	:	Poly(5-carboxyindole)
CQ	:	Chloroquine
CQDs	:	Carbon quantum dots
CV	:	Cyclic voltammetry
Cys	:	L-Cysteine
D	:	Diffusion coefficient
DA	:	Dopamine
DI	:	Deionised
DPV	:	Differential pulse voltammetry
EDS/ EDAX	:	Energy dispersive X-ray spectroscopy
EIS	:	Electrochemical impedance spectroscopy
eV	:	Electron volt
FTIR	:	Fourier transform infrared
GCE	:	Glassy carbon electrode
g-C ₃ N ₄	:	Graphitic carbon nitride
GNR	:	Gold nanorods
GO	:	Graphene oxide
GQDs	:	Graphene quantum dots
h / hr	:	Hour(s)
H ₂ O ₂	:	Hydrogen peroxide
HER	:	Hydrogen evolution reaction
HPLC	:	High performance liquid chromatography
HR-TEM	:	High resolution transmission electron

LIST OF ABBREVIATIONS

		microscopy
LoD	:	Limit of Detection
LSV	:	Linear sweep voltammetry
Min	:	Minute(s)
mM	:	millimolar
MoS ₂	:	Molybdenum disulphide
MoS ₂ -CPIIn	:	Poly(5-carboxyindole) stabilized molybdenum disulphide nanosheets
MoS ₂ -GNR	:	Gold nano rods decorated molybdenum disulphide nanosheets
ms	:	Millisecond(s)
nM	:	Nanomolar
nm	:	nanometer
NPs	:	Nanoparticles
NVP	:	Nevirapine
PANI	:	Polyaniline
PBS	:	Phosphate buffer solution
Pd NPs	:	Palladium nanoparticles
Pd@rGO	:	Palladium nanoparticles in reduced Graphene oxide matrix
PIn	:	Polyindole
PPy	:	Polypyrrole
PQ	:	Primaquine
Pt NPs	:	Platinum nanoparticles
R ²	:	Regression coefficient value
R _{ct}	:	Charge transfer resistance
RE	:	Reference electrode
RT	:	Room temperature

LIST OF ABBREVIATIONS

rGO	:	Reduced graphene oxide
rGO@WS ₂ QDs	:	Tungsten disulphide quantum dots decorated graphene oxide
RSD	:	Relative standard deviation
RT	:	Room temperature
s	:	Second
SAED	:	Selected area electron diffraction pattern
S/N	:	Signal to noise ration
SEM	:	Scanning electron microscopy
SPE	:	Screen printed electrode
SWV	:	Square wave voltammetry
T	:	Temperature
TEM	:	Transmission electron microscopy
TP	:	Theophylline
TMDs	:	Transition metal dichalcogenides
UA	:	Uric acid
UV–Vis	:	UV Visible
V	:	Volt
VAN	:	Vanillin
WE	:	Working electrode
WS ₂ QDs	:	Tungsten disulfide quantum dots
XPS	:	X–ray photoelectron spectroscopy
XRD	:	X-ray diffraction

Preface

In the present scenario, most of the countries worldwide are facing the burden of various communicable and non-communicable diseases. However, developing countries like India are more vulnerable and more exposed because of multiple factors including demographic, socioeconomic, and geographic factors.

Various lethal diseases are prevalent across the world like Cancer, HIV infection, Malaria, TB, etc. which are responsible for high mortality rates. Several therapeutic drugs are used for the treatment and cure of these diseases. These drugs function effectively and positively when they are present in the human body within a particular concentration window. The amount of drug present in the body is essential to be determined because if the concentration of the drug would be lesser than the appropriate amount, the cure of the disease would be difficult and if the concentration of the drug is higher than the desired amount (due to the drug overdose), it would prove to be fatal and severe adverse symptoms could be observed, and it may lead to death in severe cases. So, there is a need for a cheap, sensitive, and accurate sensor so that the concentration of the drug and its by-products can be quantitatively estimated in the patient's blood on a real-time basis.

A sensor is a device that detects a change in the environment or change on account of the interaction of the analyte and thereby converts it into a readable output signal. We are surrounded by a large number of sensors in our daily life, and they can broadly be categorized into chemical, physical, and biosensors. A physical sensor transforms a physical quantity like temperature, pressure, mass, etc. into a signal. A chemical sensor detects a chemical substance by chemical or physical responses and transforms it into a signal. Similarly, a biosensor detects chemical substance by using a biological sensing element.

Preface

Basically, a sensor is composed of two important components *viz.* an active layer or the recognition and a transducer. Herein, the active layer (or the recognition layer) represents the heart of a sensor, while the transducer converts the change in the environment into an observable signal such as optical, electrochemical, electrical, etc. On the basis of the method of transduction, the sensor can be categorized into physical, chemical, and electrochemical sensors. In this thesis, we have focused on electrochemical sensors since they are associated with a large number of advantages such as excellent sensitivity, high selectivity, great reproducibility, high stability and portability, and they are easy to operate and economical. In electrochemical sensing, the electrode surface acts as the active layer of the sensor. Efforts are made to synthesize such materials for electrode modification that enhance the efficacy of an electrochemical sensor. These electrode materials include a variety of materials such as polymeric materials, composites, metal complexes, nanomaterials, etc. Among them, nanomaterials present themselves as one of the best choices nowadays because they offer high sensitivity due to great surface-to-volume ratio, rapid electrode kinetics, good catalytic activity, easy functionalization, excellent biocompatibility, etc. On the basis of confinement of directional movement of electrons, nanomaterials are mainly categorized into zero, one, two and three-dimensional nanomaterials. Among these, 2D nanomaterials have regarded as a large number of applications in diverse fields due to their intriguing mechanical, electrical, and thermal properties. However, it possessed tendency to aggregate which reduces their efficacy due to a decrease in the active surface area and the number of active sites. The problem of aggregation can be overcome by a composite formation with other nanomaterials such as metal nanoparticles, metal oxide nanoparticles, polymers, other 2D materials, quantum dots, etc. resulting in the enhancement in the desired properties of these materials.

Preface

The main focus of the thesis is to synthesize and characterize the composites of 2D nanomaterials with transition metal dichalcogenides quantum dots (WS₂ QD), conducting polymer (5-carboxypolyindole), and metal nanostructure (gold nanorods). Thereafter, employing the as-synthesized nanocomposites for the modification of commercially available glassy carbon electrodes for voltammetric sensing of various therapeutic drugs like Primaquine, Chloroquine administered to patients suffering from malarial disease, and an immunosuppressive drug, Azathioprine. Thus, on these views, the therapeutic drugs are selected as target analytes in our case of research work, and voltammetric sensors are designed for the trace-level detection of these drugs. Some antimalarial drugs and an anti-inflammatory drug are chosen as target analytes, prolonged exposure of which can cause severe adverse effects on the health and may also prove to be lethal. All work in the thesis has been fractionated into six chapters as following manner:

Chapter 1 pertains to the general terminologies related to the research works like concepts of sensors, categories of sensors, components of sensors, electrochemical sensors and their superiority over other sensors, the importance of nanomaterials and their advantages, transition metal dichalcogenides and their composites for electrochemical sensing applications, the need to produce the sensor for drugs related to harmful diseases and abnormalities. At last, it also includes the literature survey based on the proposed research topic

Chapter 2 illustrates the various experimental techniques utilized for characterizing the synthesized materials. The major techniques that have been employed for the characterizations include Transmission Electron Microscopy (TEM), Scanning Electron Microscopy (SEM), X-ray Diffraction (XRD), Energy Dispersive Spectroscopy (EDX),

Preface

X-ray photoelectron spectroscopy (XPS), and Fourier Transform Infrared Spectroscopy (FTIR) for the structural and morphological investigations. UV-Visible spectroscopy (UV-vis) has been used employed for spectroscopic characterizations. Cyclic Voltammetry (CV), Differential Pulse Voltammetry (DPV), and Electrochemical Impedance Spectroscopy (EIS) have been utilized for electrochemical characterization and sensing of the analytes.

Chapter 3 presents the development of trace level sensor for an antimalarial drug-Chloroquine (CQ) on the tungsten disulfide quantum dots decorated reduced graphene oxide sheets (rGO@WS₂ QDs) modified glassy carbon electrode (GCE) surface. Prior to the trace analysis, this chapter explains about the synthesis of rGO@WS₂ QDs composite and its characterization by UV-Vis., TEM, SEM, EDS, and FTIR. At last, this conducting matrix has shown for excellent electroactivity, high catalytic property, and rapid electron transfer kinetics. CV and DPV were employed for the quantitative determination of CQ in phosphate buffer, human blood serum, and commercially available CQ tablets. The obtained analytical parameters are found to be comparable to or better than previously reported CQ sensors. The proposed sensor is very much sensitive, stable, reproducible, and selective for CQ detection and with great potential for real-time CQ sensing in malarial patients.

Chapter 4 presents an electrochemical sensor based on molybdenum disulfide nanosheets modified with poly(5-carboxyindole) (MoS₂-CPIIn) for the trace-level detection of an anti-inflammatory drug Azathioprine (Azp) through DPV. MoS₂ nanosheet has been synthesized through hydrothermal synthesis and characterized by XRD, TEM, SEM, EDS, and FTIR. Further, CPIIn chains were grown over the MoS₂ nanosheets to obtain the MoS₂-CPIIn composite. Azp was determined in phosphate

Preface

buffer as well as human blood serum at room temperature. The developed sensor demonstrates an extensively wide linear range and a low limit of detection. The developed sensor shows excellent stability, sensitivity, and good selectivity at physiological pH. The achieved analytical parameters are found to be comparable to or better than previously reported CQ sensors.

Chapter 5 presents an electrochemical sensor based on gold nanorods decorated molybdenum disulfide nanosheets (MoS₂-GNR) for the quantitative estimation of an anti-malarial drug Primaquine (PQ) through DPV. GNR was synthesized through a seed-mediated growth methodology and characterized by XRD, TEM, EDS and FTIR. Further, GNR were decorated over the MoS₂ nanosheets to obtain the MoS₂-GNR composite which possesses excellent electroactivity, high catalytic properties, and rapid electron transfer kinetics. PQ sensing was validated in phosphate buffer, human blood serum, and commercially available PQ tablet. The proposed electrochemical sensor shows a wide concentration range and a low limit of detection and offers a fascinating sensitivity, selectivity, stability, and reproducibility at physiological pH conditions with great potential to be used as a detection tool in diagnostic centers. The analytical parameters obtained are found to be comparable to or better than previously reported PQ sensors.

Chapter 6 includes the conclusive remarks and future prospects of the thesis.

CONTENTS

		Page No
List of Figures		i-vi
List of Tables		vii
List of Abbreviations / Symbols		viii-xi
Preface		xii-xvi
Chapter – 1	Introduction & Literature Survey	1-44
	1.1 General Introduction	1
	1.2 Classification based on Transducers	2
	1.3 Classification based on receptors/recognition layer	8
	1.4 Parameters of a sensor	12
	1.5 Advantages of electrochemical sensors	14
	1.6 Convenient techniques employed for modification of electrode	15
	1.7 Nanomaterials	17
	1.8 Nanocomposites of 2D materials	24
	1.9 2D Nanomaterials and their nanocomposites in Drug sensing applications	32
	1.10 Motivation and Objective of the thesis	40
	1.11 Advantages of developed materials for sensing applications	42
Chapter – 2	Experimental Techniques	45-66
	2.1 Characterization Techniques	45
Chapter – 3	Voltammetric determination of the antimalarial drug chloroquine using a glassy carbon electrode modified with reduced graphene oxide on WS₂ quantum dots	67-86
	3.1 Introduction	67
	3.2 Experimental Section	69
	3.3 Results and Discussion	73
	3.4 Conclusions	86
Chapter – 4	Immunosuppressive Drug Sensor based on MoS₂-Polycarboxyindole Modified Electrodes	87-108
	4.1 Introduction	87
	4.2 Experimental Section	90
	4.3 Results and Discussion	94
	4.4 Conclusions	107
Chapter – 5	Electrochemical detection of antimalarial drug Primaquine based on MoS₂ nanosheets - gold nanorods nanocomposite modified electrode	109-134

CONTENTS

	5.1 Introduction	109
	5.2 Experimental Section	113
	5.3 Results and Discussion	117
	5.4 Conclusions	134
Chapter – 6	Summary and Future Work	135-139
References		140-165
List of Publications		